

# Propagation of a Magnetic Domain Wall in a Submicrometer Magnetic Wire

T. Ono,<sup>1\*</sup> H. Miyajima,<sup>1</sup> K. Shigeto,<sup>2</sup> K. Mibu,<sup>2</sup>  
N. Hosoi,<sup>2</sup> T. Shinjo<sup>2</sup>

The motion of a magnetic domain wall in a submicrometer magnetic wire was detected by use of the giant magnetoresistance effect. Magnetization reversal in a submicrometer magnetic wire takes place by the propagation of a magnetic domain wall, which can be treated as a "particle." The propagation velocity of the magnetic domain wall was determined as a function of the applied magnetic field.

Recent developments of nanolithography techniques make it possible to prepare submicrometer dots and wires with well-defined shape, which has helped spur studies of the quantum phenomena in mesoscopic magnetic materials such as macroscopic quantum tunneling (MQT) and macroscopic quantum coherence (MQC) (1). Depinning of a magnetic domain wall from the pinning center in ferromagnetic (FM) narrow wires occurring through MQT has been discussed from both experimental (2) and theoretical (3) viewpoints. Investigation of this problem requires detection of magnetic domain wall motion in the wire. Because of the small particle volume, however, magnetization ( $M$ ) measurements of mesoscopic magnetic materials were, in general, limited to samples consisting of a huge number of presumably identical particles or wires. As a result, the essential magnetic properties of a single particle or a single wire were masked by the inevitable distribution of size or shape. Experimental studies of an individual magnetic particle or wire in a submicrometer range have become possible with the development of techniques such as magnetic force microscopy (4), electron holography (5), Lorenz microscopy (6), and micro-superconducting quantum interference device magnetometry (7). Up to now, however, quantitative measurements (such as velocity estimation) on dynamical properties of a domain wall in a submicrometer magnetic wire have proved very difficult.

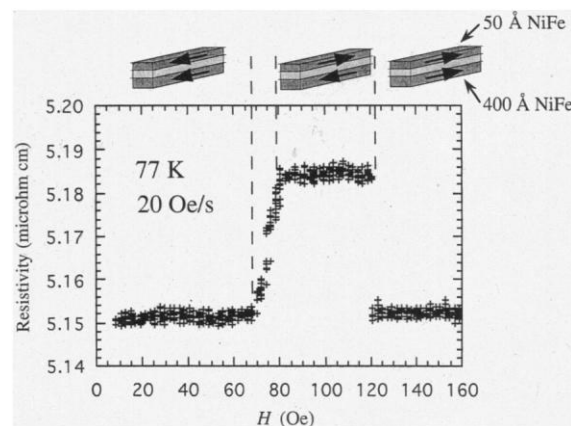
In a very narrow FM wire, the  $M$  is restricted to be directed parallel to the wire axis because of the magnetic shape anisotropy. Normally, it is considered that the  $M$  reversal takes place by nucleation and propagation of the magnetic domain wall, which lies in a plane perpendicular to the wire axis. The

process of  $M$  reversal is especially interesting at low temperatures, where the MQT process may dominate. Direct measurement of  $M$  in a submicrometer magnetic wire, however, is difficult because the volume is very small.

We studied the  $M$  reversal in a single submicrometer magnetic wire based on a non-coupled-type giant magnetoresistance (GMR) effect. The GMR is the electrical resistance change caused by the change of the magnetic structure in multilayers (8). Thus, the magnetic structure of the system can be detected by resistivity ( $\rho$ ) measurements. Especially in the case of wire composed of FM/nonmagnetic/FM layers, the GMR change is directly proportional to  $M$  in one of the FM layers. As we reported (9), it is possible to detect a very small change in  $M$  in a single NiFe/Cu/NiFe trilayer wire (thicknesses of 200, 100, and 50 Å, respectively) with 0.5  $\mu\text{m}$  width by the GMR effect. The time variation of the resistance during the  $M$  reversal reveals how the magnetic domain wall propagates in the wire (10).

The magnetic field  $H$  was applied along the wire axis, and  $\rho$  was determined using a four-point dc technique. An electrical current flowing in a sample was supplied by a battery (1.5 V) to minimize the noise from a current source. The magnitude of the electrical current was adjusted by using a proper resistance

**Fig. 1.** Resistance as a function of the external magnetic field at 77 K determined by a four-point dc technique. The resistance was measured at 10-ms intervals, while sweeping the field at a rate of 20 Oe/s. The magnetic domain structures inferred from the resistance measurement are schematically shown.



in the circuit. The typical current was 100  $\mu\text{A}$ . The voltage across two voltage probes was monitored by a differential preamplifier (LeCroy DA1855) and an 8-bit digital oscilloscope (LeCroy 9310), with  $1 \times 10^8$  per second sampling rate and 400-MHz bandwidth. The current passing through the magnet was also monitored by the digital oscilloscope so as to simultaneously obtain resistance and applied magnetic field during the  $M$  reversal.

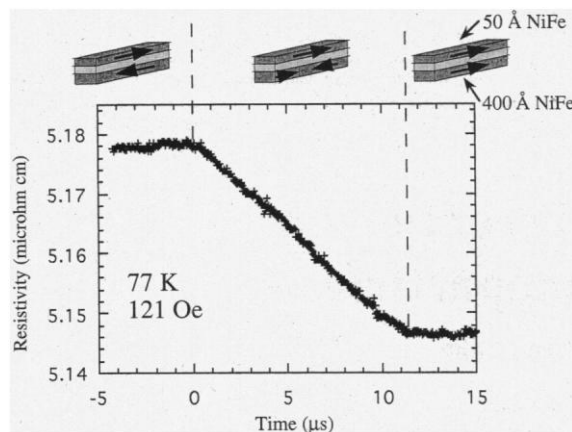
The resistance change of the trilayer system at 77 K is shown as a function of the applied magnetic field (Fig. 1). Before the measurement, a magnetic field of 500 Oe was applied in order to align  $M$  in one direction. Then the resistance was measured at 10-ms intervals, while sweeping the field toward the counter direction at a rate of 20 Oe/s. As far as the counter field being smaller than a critical field (70 Oe), both  $M$  values in two NiFe layers are aligned in parallel and the resistance takes the smallest value. When the applied magnetic field exceeds 70 Oe, the resistance rises and stays at the largest value until the field reaches 120 Oe, when the resistance abruptly decreases to the smallest value. The result indicates that the antiparallel  $M$  alignment is realized in the field range between 80 and 120 Oe, where the resistance shows the largest value. We have evidence from a preliminary study of NiFe wire arrays deposited onto V-groove substrates in the thickness range described here indicating that the thicker NiFe layer has a larger coercive force than the thinner one (11). Therefore, the change in resistance at 80 and 120 Oe is attributed to the  $M$  reversals of the 50 Å NiFe and 400 Å NiFe layers, respectively. Because we did not find any measured point during the  $M$  reversal of the 400 Å NiFe layer (Fig. 1), we conclude that the  $M$  reversal of the 400 Å NiFe layer is completed within 10 ms. However, the  $M$  reversal of the 50 Å NiFe layer gradually proceeds with increase of the applied magnetic field. This result indicates that the  $M$  reversal of the 50 Å NiFe layer takes place by the pinning and depinning of

<sup>1</sup>Faculty of Science and Technology, Keio University, Yokohama 223-8522, Japan. <sup>2</sup>Institute for Chemical Research, Kyoto University, Uji 611-0011, Japan.

\*To whom correspondence should be addressed. E-mail: teruo@phys.keio.ac.jp

## REPORTS

**Fig. 2.** Time variation of the resistance during the  $M$  reversal of the 400-Å NiFe layer at 77 K, which was collected at 40-ns intervals. The applied magnetic field simultaneously monitored by digital oscilloscope was 121 Oe. Because the sweeping rate of the applied magnetic field was 20 Oe/s, the variation of the applied magnetic field during  $M$  reversal was less than  $2 \times 10^{-5}$  Oe. Thus, the applied magnetic field is regarded as constant during the measurements.



the magnetic domain wall. Hereafter, we focus on the  $M$  reversal of the NiFe layer of 400 Å thickness.

An experimental result is shown for the time variation of the resistance during the  $M$  reversal in the 400 Å NiFe layer (Fig. 2). The data were collected at 40-ns intervals. The linear variation of resistance with time in Fig. 2 indicates that the propagation velocity of the magnetic domain wall is constant during the  $M$  reversal of the 400 Å NiFe layer. This constant velocity suggests that the  $M$  reversal takes place by the propagation of a single magnetic domain wall, the propagation velocity of which at the applied field of 121 Oe is estimated to be 182 m/s from the time (11 μs) of the wall traveling across the two voltage probes (2 mm). Because the sweeping rate of the applied magnetic field was 20 Oe/s, the variation of  $H$  during  $M$  reversal is less than  $2 \times 10^{-5}$  Oe. Thus,  $H$  is regarded as constant during the measurements. It should be noted that the time variation of resistance can be converted into the time variation of domain wall position in the wire, because the domain wall comes from one of two voltage probes and runs toward the other voltage probe. Therefore, the domain wall position as a function of time can be obtained by this method.

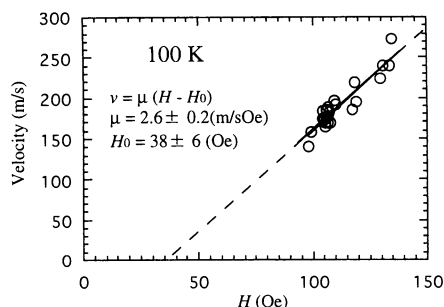


**Fig. 3.** Dependence of domain wall velocity  $v$  on amplitude  $H$  of the applied magnetic field at 100 K. The wall velocity depends linearly on the applied magnetic field and is described as  $v = \mu(H - H_0)$ , where  $\mu = 2.6 \pm 0.2$  m/sOe and  $H_0 = 38 \pm 6$  Oe.

Because the reversal field of the 400 Å NiFe layer fluctuated from run to run in the range of 90 to 140 Oe, the wall velocities at various  $H$ 's were obtained by repeating the measurements shown in Fig. 2. The result at 100 K is shown in Fig. 3. The wall velocity depends linearly on  $H$  and is described as  $v = \mu(H - H_0)$ , where  $v$  is the wall velocity and  $\mu$  is the so-called wall mobility; it was obtained that  $\mu = 2.6 \pm 0.2$  m/sOe and  $H_0 = 38 \pm 6$  Oe. This mobility is much less than that obtained for a NiFe film with the same thickness (12). Figure 4 shows the temperature ( $T$ ) dependence of mobility ( $\mu$ ) and  $H_0$ .  $H_0$  is considered to be the field below which the magnetic domain wall cannot propagate because of the pinning by structural defects. Therefore, the decrease of  $H_0$  with increase of  $T$  (Fig. 4) can be interpreted as a thermal-assisted effect. In contrast, the wall mobility is almost constant in the range from 100 to 160 K. When the wall mobility is limited by eddy currents, the mobility is described as  $\mu = C\rho/M_s d$ , where  $C$  is constant,  $M_s$  is the saturation, and  $d$  is the film thickness (13). Therefore, the mobility should increase with increase of temperature, because  $\rho$  increases and  $M_s$  decreases with an increase of  $T$ . Moreover, the rough estimation of the mobility, assuming a rigid wall, gives  $\mu = 1.6 \times$

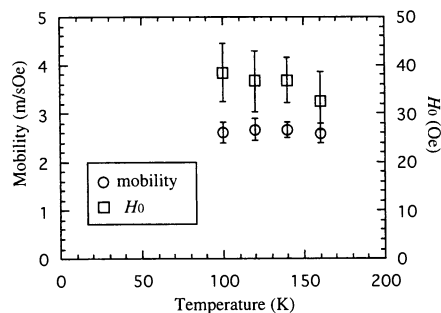


**Fig. 4.** Temperature dependence of mobility  $\mu$  and  $H_0$ . Whereas  $H_0$  decreases with an increase of temperature, the wall mobility is almost constant in the temperature range from 100 to 160 K.

$10^4$  m/sOe for the 400 Å NiFe film (13). This value is three orders of magnitude larger than the experimentally obtained value. Therefore, the experimentally obtained mobility cannot be explained by the eddy currents loss. The other mechanism which limits the wall mobility is the Gilbert damping. If we assume a flat domain wall with a continuous internal spin structure, the wall mobility expresses theoretically as  $\mu = \gamma\Delta/\alpha$  (14), where  $\gamma$  is the gyromagnetic ratio,  $\Delta$  is the domain wall width, and  $\alpha$  is the Gilbert damping parameter. By using the experimentally obtained value of  $\mu$  and assuming  $\Delta = 100$  nm,  $\alpha = 0.63$  is obtained. Although this value is greater than that estimated from the width of the FM resonance line (12), such large  $\alpha$  values have also been reported in ultrathin Co films (15) and were attributed to the presence of defects at the surface and interface. The edge effect should also be taken into account in the case of magnetic wires. As a consequence, we conclude that the mobility is dominantly limited by Gilbert damping.

Our experiments describe a method to observe the magnetic domain wall propagation in a single submicrometer wire, and this method, as far as the resistance can be measured, can be applied to narrower wires in which the volume of the magnetic domain wall is smaller. Therefore, this method opens the way to addressing other interesting problems, such as one-dimensional propagation of a magnetic domain wall as a soliton and MQT by depinning of a magnetic domain wall from a pinning center.

### References and Notes

1. For a review of MQT/MQC, see, for example, E. M. Chudnovsky and J. Tejada, *Macroscopic Quantum Tunneling of the Magnetic Moment* (Cambridge Univ. Press, New York, 1998).
2. N. Giordano and J. D. Monnier, *Physica B* **194-196**, 1009 (1994).
3. G. Tatara and H. Fukuyama, *Phys. Rev. Lett.* **72**, 772 (1994).
4. T. Chang and J. G. Zhu, *J. Appl. Phys.* **75**, 5553 (1994).
5. T. Hirayama, Q. Ru, T. Tanji, A. Tonomura, *Appl. Phys. Lett.* **63**, 418 (1993).
6. Y. Otani et al., *Mater. Res. Soc. Symp. Proc.* **475**, 215 (1997).
7. W. Wernsdorfer et al., *Phys. Rev. Lett.* **77**, 1873 (1996).
8. M. N. Baibich et al., *ibid.* **61**, 2472 (1988).
9. T. Ono, H. Miyajima, K. Shigetani, T. Shinjo, *Appl. Phys. Lett.* **72**, 1116 (1998).
10. The samples were prepared by using lift-off techniques as follows: First, a 0.1 μm thickness of ZEP520 resist was spin-coated on a Si(100) substrate. After the pattern of wire was exposed by an electron-beam writer, the resist was developed. The NiFe(400 Å)/Cu(200 Å)/NiFe(50 Å) trilayer film was deposited on the patterned mask by electron-beam evaporation in a vacuum of  $1 \times 10^{-8}$  Torr. The wire with trilayered structure was obtained after the resist mask was removed. Because of the large Cu-layer thickness, the interlayer exchange coupling between the NiFe layers is negligible. The width of the wire is 0.5 μm, and the sample has four current-voltage terminals, where the voltage is probed over a distance of 2 mm.
11. Y. Sugita, T. Ono, T. Shinjo, unpublished results.
12. R. V. Telesin et al., *IEEE Trans. Magn.* **5**, 232 (1969).

13. G. Bertotti, *Hysteresis in Magnetism* (Academic Press, New York, 1998).
14. A. P. Malozemoff and J. C. Slonczewski, *Magnetic Domain Wall in Bubble Materials* (Academic Press, New York, 1979).
15. Kirilyuk *et al.*, *J. Magn. Magn. Mater.* **171**, 45 (1997).
16. We thank Y. Otani and R. Haßdorf for valuable discussions and N. Osada for experimental assistance. Supported by a grant-in-aid for scientific research on priority area from Monbusho in Japan.

15 December 1998; accepted 23 February 1999

## Magnetization Directions of Individual Nanoparticles

S. A. Majetich\* and Y. Jin

The magnetization directions of individual monodomain nanoparticles as small as 5 nanometers in diameter are determined using the Foucault method of Lorentz microscopy. A model is developed to explain the images and diffraction patterns of samarium cobalt nanoparticles as a function of the aperture shift direction. Thermally induced changes in the magnetization direction of superparamagnetic magnetite nanoparticles were observed but with a much slower rate than expected, due to surface anisotropy. When the time scale for magnetization reversal is much shorter than the data acquisition time, as in carbon-coated iron cobalt alloy nanoparticles, the images show an average of such thermally induced changes.

The ability to determine the magnetization direction of a monodomain nanoparticle is of great interest, particularly as the bit density of magnetic recording media is increased. In particulate media, a threshold is reached when the size of the particles or uncoupled grains approaches the superparamagnetic limit (1), which is  $\sim 10$  nm for Co. Below this size, thermal fluctuations are sufficient to change the magnetization direction, and the ability to store information is lost. The maximum size for superparamagnetic behavior, below which the magnetization reversal field or coercivity  $H_c$  drops to zero, and the maximum monodomain size, where  $H_c$  is maximized, can be estimated for different materials (2–4). However, the predictions fail for compounds with either very high or very low magnetocrystalline anisotropy (5, 6). The Stoner-Wohlfarth theory (7) predicts the size-dependent coercivity for isolated ellipsoidal monodomain particles, but the experimental  $H_c$  is always lower, a result known as Brown's Paradox (8).

We report the extension of Lorentz microscopy to determine the magnetization direction in  $\text{SmCo}_5$ ,  $\text{Fe}_3\text{O}_4$ , and carbon-coated  $\text{Fe}_{50}\text{Co}_{50}$  nanoparticles as small as 5 nm. Although micro-SQUIDS (superconducting quantum interference devices) (9, 10) enable the magnetization  $M$  to be determined quantitatively, it is difficult to study a large number of different particles individually. Alternatively, magnetization directions can be determined by Lorentz microscopy and magnetic force microscopy (MFM). In order to

realize the quantum disk (11), where each particle is an individual bit, a nondestructive method such as MFM would be required. However, for features smaller than 100 nm, Lorentz microscopy is currently superior (12), and this technique was therefore used in this study.

Two types of Lorentz microscopy have previously been used to study small particles, the Fresnel and Foucault methods. In the Fresnel method (13), the sample is imaged with the plane of focus above or below the specimen. Where  $M$  of the sample is changing, such as in the domain walls of a thin film, electron trajectories either converge or diverge and appear as bright or dark regions in the image, respectively. Hütten *et al.* (14) investigated Co precipitates with particle diameters of 50 to 100 nm in  $\text{Au}_{72}\text{Co}_{28}$  alloy thin films and compared the images with simulations based on electron trajectories. The spherical particles appeared either entirely bright or entirely dark and reversed their contrast between underfocus and overfocus conditions. The particles were first modeled as single domains, with a varying magnetization direction with respect to the vertical axis. These simulations predicted asymmetric images, in contrast to the actual observations. A modified model assumed magnetization reversal by curling, with no external fringe field. Contrast dependent only on the curling direction of the particle magnetic induction relative to the incident electron velocities was used to explain the experimental observations of bright and dark spots at the locations of the Co particles.

Foucault method Lorentz microscopy was done by Salling *et al.* (15) on needle-shaped  $\gamma\text{-Fe}_2\text{O}_3$  particles on the order of 65 nm in

diameter and 300 nm in length. In the Foucault method (16), the objective aperture is shifted to block electrons that have passed through parts of the sample magnetized in a particular direction, causing these regions to appear dark in the resulting image. This aperture is located in the back focal plane of the objective lens, where the electron intensity is in the form of the diffraction pattern for the sample. For a thin film containing two domains with opposite  $M$  values, shifting the aperture can make one entire domain dark and the other bright, or vice versa, depending on the direction of the shift. The fine particles of  $\gamma\text{-Fe}_2\text{O}_3$  were magnetized along the long axis, and when the aperture was shifted, dark lobes appeared on both sides of the particle, which were attributed to the fringe field. When the same particle was magnetized in the opposite direction, no dark lobes were visible, and the particle appeared the same as in the bright-field image.

We extend the size range to even smaller particles, some of which are below the superparamagnetic limit, and present a model for interpreting the images. First, the Foucault Lorentz microscopy method was used to image nanoparticles of the high anisotropy alloy  $\text{SmCo}_5$ , revealing features not observed in the larger, elongated particles studied by Salling *et al.* (15). Details of the preparation of these ball-milled nanoparticles have been reported elsewhere (17). In this material, the superparamagnetic limit is 2 nm, and larger particles are expected to have stable magnetization directions. The results as a function of the aperture shift direction provide the basis for interpreting the Lorentz microscopy images of extremely small particles. Next, this method was applied to two systems expected to contain superparamagnetic particles:  $\text{Fe}_3\text{O}_4$  nanoparticles from a ferrofluid (18) (EMG-705; Ferrofluidics Corp., Nashua, New Hampshire) and carbon-coated  $\text{Fe}_{50}\text{Co}_{50}$  nanoparticles made in a plasma torch (19). Although magnetization reversal occurs on a nanosecond time scale and the dynamics are not observed directly, particles may exist in metastable states for minutes or even hours between thermal switching events (20).

Foucault Lorentz microscopy was carried out in a JEM-120CX (JEOL, Sundbyberg, Sweden) transmission electron microscope (TEM) with a Lorentz pole piece, so that the sample was loaded into a magnetic field-free region. Lorentz microscopy was also performed using a JEOL 4000 EX electron microscope equipped with a Gatan imaging energy filter and used with an objective minilens in order to keep the sample in a field-free region. The particles were examined under bright-field conditions, and then the objective aperture was shifted to cut off part of the electron beam transmitted by the sample. Images of  $\text{SmCo}_5$  nanoparticles were recorded for a series of different aperture shift direc-

Department of Physics, Carnegie Mellon University, Pittsburgh, PA 15213-3890, USA.

\*To whom correspondence should be addressed. E-mail: sm70@andrew.cmu.edu